Effect of Polydispersity on the Self-Assembly Structure of Diblock Copolymers under Various Confined States: A Monte Carlo Study

Yuanyuan Han, Jie Cui, and Wei Jiang*

State Key Laboratory of Polymer Physics and Chemistry, Changchun Institute of Applied Chemistry, Chinese Academy of Sciences, Changchun 130022, P. R. China, and Graduate School of the Chinese Academy of Sciences

Received August 18, 2007; Revised Manuscript Received June 4, 2008

ABSTRACT: We studied the self-assembly of polydisperse diblock copolymers under various confined states by Monte Carlo simulation. When the copolymers were confined within two parallel walls, it was found that the ordered strip structures appeared alternately with the increase in wall width. Moreover, the wall width at which the ordered structure appeared tended to increase with an increase in the polydispersity index (PDI). On the other hand, the simulation results showed that the copolymers were likely to form ordered concentric strip structures when they were confined within a circle wall. An increase in the PDI led to a change in structure from an ordered concentric strip structure to a newly ordered concentric strip structure. It is interesting to note that one strip was lost while the center was replaced by the other component as the PDI increased. Similar results were obtained in the case of three dimensions. That is, the copolymers were confined in a spherical or cylindrical space. Further along, one layer was lost, and the core was occupied by the other component with the increase in the PDI. We illustrated these phenomena in terms of the frustration between the bulk lamellar repeat period and the confined spacing.

1. Introduction

Diblock copolymers that consist of two chemically distinct polymer chains (blocks) linked by a covalent bond at one end are renowned for their ability to partition chemically immiscible components into nanoscale domains. These domains often exhibit intriguing complex periodic geometries with long-range order.[1] A variety of ordered bulk phases is observed for diblock copolymers such as lamellae, hexagonally packed cylinders, and body-centered-cubic spheres.[2] In a physically confined environment, structural frustration, confinement-induced entropy loss, and surface interactions can strongly influence the molecular organization which is vital to the morphology formed in the final output.

In recent years, therefore, the phase behaviors of diblock copolymer melts in confined states have been considered an important topic by both theorists[3–18] and experimentalists.[19–25] Liang et al. systematically investigated the morphologies of symmetric[7] and asymmetric[14] diblock copolymers under cylindrical confinement. A variety of morphologies including stacked-disk, single-helix, catenoid-cylinder, gyroidal, and stacked-circle structures were observed when varying the strength of the surface interactions in the case of symmetric diblock copolymers. Likewise, a rich variety of structures, such as helices, stacked toroids, and perforated tubes, was observed as a function of the degree of confinement as well as the strength of surface interactions in the case of asymmetric diblock copolymers. Yu et al. studied the dependence of the self-assembled morphologies and chain conformations on the degree of confinement and the strength of the surface interactions.[8,15,16] More recently, Zhu and Jiang[12] studied the self-assembly of diblock copolymer mixtures (A-*b*-B/A-*b*-C or A-*b*-B/B-*b*-C mixtures) subjected to cylindrical confinement by using Monte Carlo simulation. Relative to the structures of the individual components, the self-assembled structures of the diblock copolymer mixtures are more complex and interesting. In a series of papers,[20–24] Russell and co-workers reported the study of symmetric and asymmetric polystyrene-*b*-polybutadiene confined within nanoscopic cylindrical pores in alumina membranes. They found that when the pore diameter is larger than the equilibrium period, a multiple set of concentric cylinders is observed. On the other hand, when these two parameters are comparable, a novel stacked-disk or toroid morphology is formed.

On the other hand, it is generally known that all synthetic copolymers are polydisperse, which can influence many properties of the copolymers, such as static and dynamic properties, phase behaviors, and the likes. A number of theoretical studies[26–35] and experimental studies[36–44] considering the polydispersity of block copolymers have appeared in various literatures. For instance, Fredrickson et al.[31] presented an algorithm to incorporate the realistic molecular weight distributions into the field theory models of inhomogeneous polymeric fluids. Afterward, this efficient algorithm was presented for numerically evaluating a self-consistent-field theoretical model of an AB diblock copolymer that incorporates continuous polydispersity in one of the blocks by them.[32] And a novel chain-segregation effect is found in which chains of intermediate molecular weight are concentrated at domain interfaces. Liang et al.[33] studied the effect of polydispersity on the formation of vesicles from amphiphilic diblock copolymers in a dilute solution using the real-space self-consistent-field theory. It was found that larger polydispersity favors the formation of smaller vesicles or quasi-vesicles, and this effect can be attributed to the segregation of copolymers according to their chain lengths. Very recently, Cooke and Shi[34] studied the influence of polydispersity on the phase behavior of diblock copolymer melts using a self-consistent-field theoretical model. It was found that the order−disorder transition boundary shifts to higher temperatures. For asymmetric polymer distributions, polydispersity favors structures with curved interfaces. The domain spacing of the ordered structures increases with a rise in polydispersity index. Ji and Ding[35] studied the formation of vesicles from mixed amphiphiles with dispersed molecular weight using Monte Carlo simulation. They found that the amphiphiles with longer hydrophilic blocks preferred to segregate into the outer monolayer of the resultant vesicles, which is consistent with

* Corresponding author: e-mail wjiang@ciac.jl.cn; Tel +86-431-85262151; Fax +86-431-85262126.

10.1021/ma800702f CCC: $40.75
Published on Web 07/25/2008

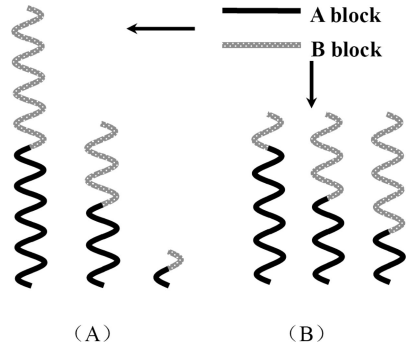

Figure 1. Schematic diagram showing the construction of the polydisperse diblock copolymers used in this study: (A) polydisperse symmetric diblock copolymer system; (B) polydisperse asymmetric diblock copolymer system.

the experimental observations in recent literature.[37,38] Moreover, Bendejacq et al.[39] obtained several polystyrene-*b*-poly(acrylic acid) diblock copolymers with broad molecular weight distributions and discovered that these systems produced well-ordered structures. It was then reported that Matsushita et al.[42,43] synthesized a series of polystyrene-*b*-poly(2-vinylpyridine) diblock copolymers with narrow molecular weight distributions. These copolymers were blended to prepare copolymer systems with different PDIs. It was found that the lamellar domain spacing increases as the PDI is increased. When PDI > 1.8, macrophase separation was observed. Recently, Lynd and Hillmyer[44] synthesized several sets of poly(ethylene-*alt*-propylene)-*b*-poly(DL-lactide) diblock copolymers with controlled molecular weights, compositions, and polydispersity indices. Small-angle X-ray scattering was used to evaluate the influence of polydispersity on the equilibrium domain spacing and resultant ordered structure. They observed that the domain spacing increases linearly with an increase in polydispersity for PDI from 1.20 to 2.00. The experiments also show that a larger PDI can lead to a change in morphology for a compositionally asymmetric diblock copolymer.

However, to the best of our knowledge, the self-assembly of confined polydisperse block copolymers has been seldom studied up to now. In this paper, Monte Carlo simulation was used to study the aggregation of confined diblock copolymers by changing the polydispersity index and boundary condition. This was done to reveal the effect of polydispersity and confined condition on the self-assembly of confined diblock copolymers.

2. Model and Simulation

The polydisperse diblock copolymer systems were constructed by blending three different symmetric diblock copolymer chains in length as shown in Figure 1A. The three copolymer chains were A_3-*b*-B_3, A_{15}-*b*-B_{15}, and A_{27}-*b*-B_{27}. We defined the lengths of these three copolymer chains as $LE_1 = 6$, $LE_2 = 30$, $LE_3 = 54$ and set the molecular weight of each unit as 1. In the simulation, we kept the diblock copolymer concentration and the number-average molecular weight ($\bar{M}_n = 30$) unchanged. We changed the weight-average molecular weight ($\bar{M}_w$) to obtain various polydisperse diblock copolymer systems. The polydispersity index (PDI) can be calculated from PDI $= \bar{M}_w/\bar{M}_n$. Table 1 shows the construction for some typical polydisperse diblock copolymer systems. On the other hand, for comparison purposes we kept the diblock chain length unchanged and changed the length of one block. In this case, the three copolymer chains were A_{25}-*b*-B_5, A_{15}-*b*-B_{15}, and A_5-*b*-B_{25} as shown in Figure 1B. The length of each chain was the same ($LE = 30$) whereas the fraction of each block was different, i.e., $f_{A1} = 0.75$, $f_{A2} = 0.50$, and $f_{A3} = 0.25$. Similarly, the polydispersity index (PDI) of each block was defined as $PDI_i = \bar{M}^i_w/\bar{M}^i_n$, where *i* referred to block A or B. In the simulation, $\bar{M}^i_n$ remained 15, and $\bar{M}^i_w$was variable in order to obtain various PDI_i. In this study, we used $PDI_A$to refer to the polydispersity of the system.

Table 1. One Construction for Different Polydisperse Diblock Copolymer Systems Used in This Study[a]

chain combination	$\bar{M}_n$	$\bar{M}_w$	PDI
0 A_3B_3 +120 $A_{15}B_{15}$+ 0 $A_{27}B_{27}$	30	30	1.0
28 A_3B_3 +64 $A_{15}B_{15}$+28 $A_{27}B_{27}$	30	39	1.3
56 A_3B_3 +8 $A_{15}B_{15}$+ 56 $A_{27}B_{27}$	30	48	1.6

[a] The total number of the chains remains constant, i.e., 120.

The lattice Monte Carlo simulation method was used in this study. The multiple-chain configurations were generated in two and three dimensions with various boundary shapes. In two-parallel-wall, circle, two-concentric-circle boundary conditions (2D) and spherical, cylindrical boundary conditions (3D), there are attractive interactions between the boundary and A blocks and repulsive interactions between the boundary and B blocks. Periodic boundary conditions were imposed in the direction that was parallel to the wall in the case of two-parallel-wall boundary in 2D and cylindrical boundary in 3D.

In two-dimensional space, the volume fraction of the diblock copolymers was fixed at 0.9 while in three-dimensional space, it was fixed at 0.7. The "single-site bond fluctuation model"[45–47] and the "vacancy diffusion algorithm"[48] were employed in these simulations. The evolution of the chain configuration was achieved by attempting random displacement of a single vacancy site to its eight nearest-neighboring site beads in two-dimensional space and to its 18 nearest-neighboring site beads in three-dimensional space. These attempted moves changed the lengths of the bonds within the chain. The chain connectivity was maintained by restricting the bond lengths to values of 1 and $\sqrt{2}$. Excluded volume interactions were enforced to assume that no more than one bead existed per lattice site. The bond crossing is forbidden. If the attempted move violated the excluded volume condition, or the no bond-crossing, or bond length restriction, it was rejected. Whether to move or not is further governed by the Metropolis rule;[49] i.e., if the energy change, ΔE, is negative, it is accepted. Otherwise, it is accepted with a probability *p* as follows:

$$p = \exp(-\Delta E/KT)$$

$\Delta E = (\Delta N_{AA}\varepsilon^*_{AA} + \Delta N_{BB}\varepsilon^*_{BB} + \Delta N_{AB}\varepsilon^*_{AB} + \Delta N_{AC}\varepsilon^*_{AC} + \Delta N_{BC}\varepsilon^*_{BC})$ is the change in energy that accompanied the attempted move, ΔN is the difference between the number of nearest-neighboring pairs of the sites occupied by monomers or by boundaries before and after the movement, ε^* is the reduced interaction energy (ε/KT) gained after the two neighboring sites are occupied by monomers or boundaries, and the subscripts A, B, and C denote monomers A, B, and boundary units, respectively.

In this study, we set $\varepsilon_{AB} = 1$, $\varepsilon_{AA} = \varepsilon_{BB} = 0$, $\varepsilon_{AC} = -1$, and $\varepsilon_{BC} = 1$, which ensure that A block is immiscible with B block, and the boundary attracts the A block and repulses the B block. First, the system was annealed in an athermal state ($1/KT = 0$) for a sufficiently long time to reach equilibrium disordered state. Then it was quenched to a new state ($1/KT = 0.5$). The process of phase separation in this state was simulated, and in all of the diagrams obtained block A is marked with black color and block B is marked with gray color.

3. Results and Discussion

In order to judge whether the systems are at the equilibrium state, the contact number (N_{AB}) was introduced into this work. The definition of N_{AB} is the average number of A and B pairs of segments within the distance of $\sqrt{2}$. Figure 2 shows the variation of N_{AB} with Monte Carlo time for the polydisperse

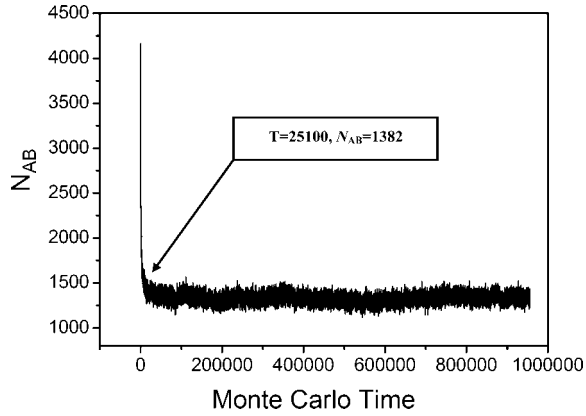

Figure 2. Variation of the contact numbers of A blocks and B blocks with Monte Carlo time for the polydisperse copolymers confined within the two-parallel-wall with a width of 75 and a length of 100. The PDI of the system is 1.6.

copolymer confined in the two-parallel-wall with a width of 75. It should be noted that N_{AB} decreases considerably with an increase in Monte Carlo time of up to about 2.5×10^4. Thereafter, it remains almost unchanged with a further increase in Monte Carlo time. To ensure that the structures are at equilibrium states, all results presented in this paper were at or above 8×10^5 Monte Carlo time.

3.1. Effect of the Polydispersity of Copolymer Chain Lengths. In this section, the length of the symmetric diblock copolymer chain is variable (as indicated in Figure 1A), but the average chain length is fixed at 30, i.e., $\bar{M}_n = 30$.

Figure 3A shows the simulation results of the structures formed by the monodisperse symmetric diblock copolymers confined within the two-parallel-wall. It is shown that the simulation results are quite consistent with the simulation results obtained by Liang et al.[6] The ordered structure appears alternately as the wall width changes. Correspondingly, Figures 3B,C show the simulation results of the structures formed by the polydisperse copolymers confined within the same boundary conditions. The polydispersity indices for these two systems are 1.3 and 1.6, respectively. From the simulation results, we can see that the structure changes from a disordered to an ordered strip structure with an increase in the wall width for both monodisperse and polydisperse systems. However, in these three systems, the ordered−disordered transitions occur asynchronously with the change of the PDI. In order to clearly show the effect of the polydispersity on the structure formed by copolymers confined in the two-parallel-wall, Figure 4 gives a diagram showing the variations of the structure with the wall width and the PDI. In this diagram, the *X* axis is the width (D) of the two-parallel-wall, while the *Y* axis is the PDI. It can be concluded that the wall width for the ordered structure tended to increase with the increase in the PDI. The first disordered−ordered transitions which appeared are at $Lx = 40$, 45, and 50 for the PDI = 1.0, 1.3, and 1.6, respectively.

It is indicated in both theory[34] and experiment[42,43] that the phase spacing (denoted by L_0) in bulk increases with increasing the PDI of the copolymers. In confined states, the self-assembled structure strongly depends on the strength of surface preference and the frustration between the size of the confinement D and L_0.[5,8,13] The present simulation study indicates that the strip period (L_0) without confinement increases correspondingly with the increase of the PDI (see Figure 1 in Supporting Information). Figure 5 shows the variation of the L_0 with the PDI. It can be concluded that the L_0 increases from 24.0 to 29.8 with the increase of the PDI from 1.0 to 1.6. Therefore, when the PDI is increased, the size of the confinement D must increase accordingly in order to maintain the commensurability of the L_0 and the size of the confinement D unchanged. This is the main reason why the ordered structure appears alternately with the change of D and the PDI (Figure 4).

Now, we changed two-parallel-wall confinements to circle confinements. Figure 6A displays the structures formed by the polydisperse symmetric diblock copolymers confined within a circle boundary with a radius of 40. We can see that the copolymers form well-ordered concentric strips when PDI = 1.0. It is clear that the phase domain sequence from the boundary to the center is A−B−A−B. With the increase in the PDI, the strip phase domains for both blocks A and B tend to become wider. However, the center phase domain tends to decrease until disappearance with an increase in the PDI from 1.0 to 1.6. Consequently, a circle strip is lost, and the center phase domain is replaced by block B; that is, the phase domain sequence from the boundary to the center becomes A−B−A in the case of PDI = 1.6. More interesting is that the aggregation still remains a well-ordered concentric strip structure. When the circle radius is increased to 50, we can see from Figure 6B that the phase domain sequence from the boundary to the center is A−B−A−B−A. Similarly, the center phase domain decreases up to disappearance, and then the center phase domain is replaced by block B with an increase in the PDI from 1.0 to 1.6. As a result, a strip is lost. In order to further probe this phenomenon, series circle boundaries with different radii and copolymer systems with different polydispersity indices are employed in this study (see Figure 2 in Supporting Information). Figure 7 is a diagram showing the structural variation with the PDI and circle radius (R) for polydisperse symmetric diblock copolymers confined within a circle boundary. It clearly shows that the copolymers are more likely to form concentric strip structures within a circle boundary. The number of strips increases with an increase in the circle radius, whereas it reduces with an increase in the PDI.

The simulation results indicate the circle confinement allows the copolymer to respond to the frustration by changing the size of the circular microdomain at the center of the system. From Figure 6 it is known that the center phase domain can decrease up to disappearance, and then the center phase domain can be replaced by block B as the PDI changes from 1.0 to 1.6. This is the main reason the circle confinement is more suitable for the polydisperse diblock copolymers to form an ordered strip structure as compared to a parallel confined boundary. In order to confirm this viewpoint, we simulated the polydisperse diblock copolymers confined within two concentric circle boundaries. The radius of the inside circle is r_0. Certainly, r_0 is invariable with the PDI. The distance between two circles, i.e., $R - r_0$, is kept as a constant. Importantly, the simulation results are quite different from those in the circle confinement. From Figure 8, it can be seen that the frustrated strip structure appears with the increase of the PDI, supporting the previous viewpoint.

Why does the center domain of block B decrease up to disappearance and the new core of block A appear with an increase in the PDI? It is known that the inner strip phase domains for both blocks A and B increases with increasing the PDI. However, the circle radius (R) remains unchanged. Therefore, the center domain should decrease in order to satisfy the increase of the strip phase domains. The center domain can become extremely small because a single block chain can likewise form a center domain. Further increasing the PDI can lead to the disappearance of the center domain, and the strip nearby the domain becomes a new center phase domain accordingly.

We also studied the polydisperse diblock copolymers confined in three dimensions. Figure 9 displays the self-assembly structures of the polydisperse copolymers confined within a spherical boundary. The copolymers' PDI ranges from 1.0 to

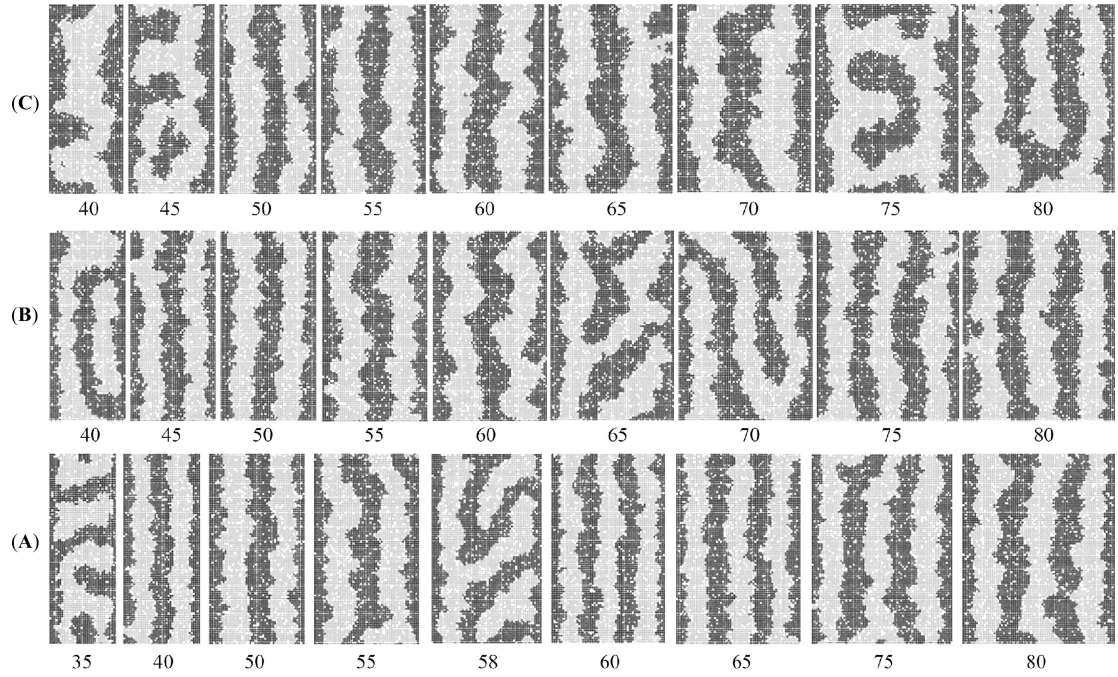

Figure 3. Snapshots of a series of polydisperse symmetric diblock copolymers confined within a two-parallel-wall with different widths. (A) PDI = 1.0, (B) PDI = 1.3, (C) PDI = 1.6. The length of the two-parallel-wall is 100, and the wall widths are marked below the snapshots correspondingly.

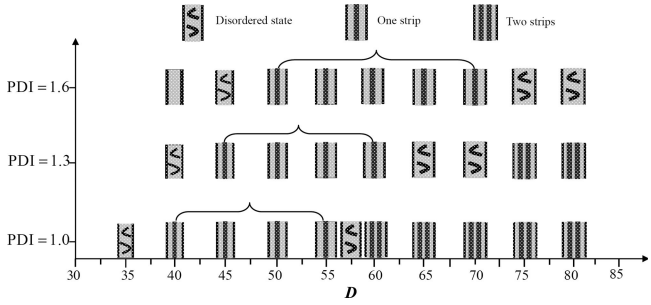

Figure 4. Diagram showing the structural variation with the PDI and wall width for polydisperse symmetric diblock copolymers confined within two-parallel-wall.

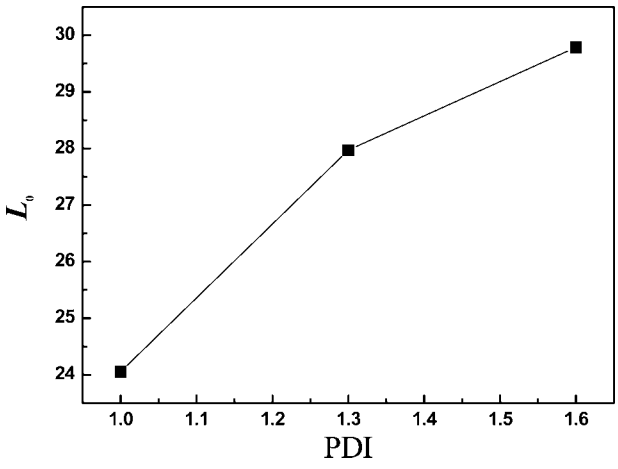

Figure 5. Variation of the strip period (L_0) under period boundary condition (i.e., without confinement) with the PDI for the symmetrical polydisperse copolymers.

1.6. We found out that the polydisperse diblock copolymers are likely to form a core−multishell structure. We likewise discovered that the phase domain sequence from the boundary to the center remains A−B−A−B−A when the PDI ranges from 1.0 to 1.4. However, the center domain decreases gradually with the increase of the PDI. While further increasing the PDI, the phase domain sequence turned to be A−B−A−B as shown in Figure 9. The core of block B disappears, and the new core of block A appears with an increase in the PDI of up to 1.5.

Figure 10 is the simulation results showing the self-assembly structures for the polydisperse copolymers confined within a cylindrical boundary. The PDI for the copolymers changes from 1.0 to 1.6. It is found that the polydisperse diblock copolymers tend to form concentric shell structures. The shell sequence is A−B−A−B from the boundary to the center in the case of PDI = 1.0 as shown in Figure 10. With the increase in the PDI, the shell sequence changes to A−B−A, and the core of block B disappears accordingly. These results are quite similar to those in the case of two dimensions; that is, the copolymers are confined within a circle. As discussed above, the variable of the size of the center domain in a wide range is the main reason that the diblock copolymers are more likely to form ordered structure within the ball or cylinder boundary.

3.2. Effect of the Polydispersity of Block Lengths. In this section, the length of each block is variable (as indicated in Figure 1B), but all the chain lengths are fixed at 30.

The simulation results of the structures formed by the polydisperse asymmetric diblock copolymers confined within a different two-parallel-wall are given in Figure 3 of the Supporting Information. The PDI_A of these two systems which were investigated is 1.2 and 1.4, respectively. Similarly, in order to study the effect of the polydispersity index (PDI_A) on the structure formed by copolymers confined within the two-parallel-wall, we give a diagram showing the structure with the wall width and the PDI_A (Figure 11).The simulation results indicate that the structure changes from a disordered to an ordered strip structure with an increase in wall width. The wall width at which the ordered structure appears tends to increase with an increase in the PDI_A. The first ordered structure which appeared is at Lx = 40, 45, and 50 for the PDI_A = 1.0, 1.2, and 1.4, respectively.

Series circle boundaries with different radii and copolymer systems with different PDI_A are employed in this study, too. All the original figures of the simulation results are given in

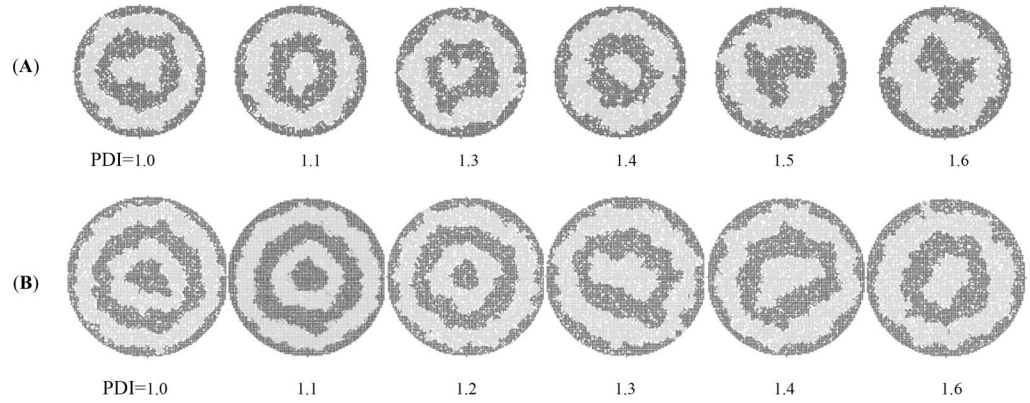

Figure 6. Snapshots of the polydisperse symmetric diblock copolymers confined within a circle boundary. Circle radius: (A) $R = 40$, (B) $R = 50$. The polydispersity indices are marked below the snapshots correspondingly.

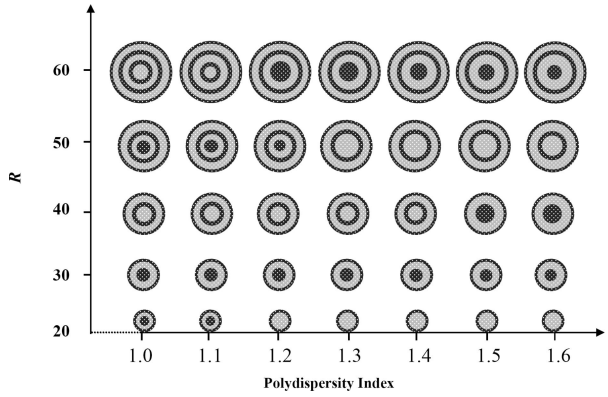

Figure 7. Diagram showing the structural variation with the PDI and circle radius (R) for polydisperse symmetric diblock copolymers confined within a circle boundary.

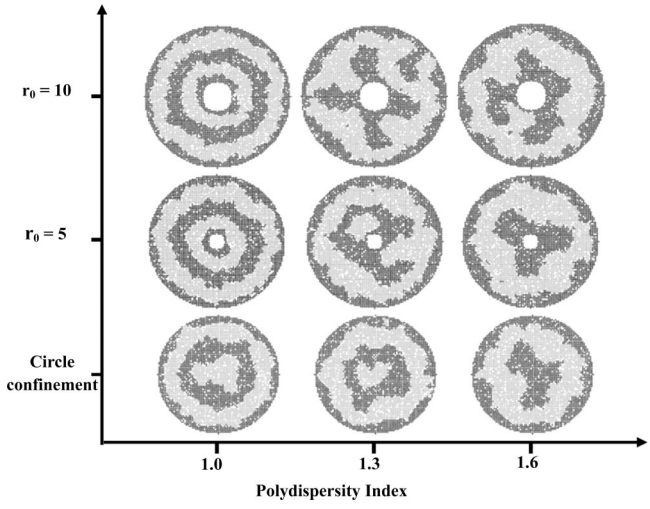

Figure 8. Snapshots of polydisperse symmetric diblock copolymers confined within two-concentric-circle boundaries with different inside radius r_0. The distance ($R - r_0$) between these two circle walls is 40. For the purpose of comparison, the simulation results for the circle confinement ($R = 40$) is given in this figure accordingly.

Figure 4 of the Supporting Information. For simplification, a diagram showing the structural variation with the PDI_A and circle radius (R) is given in Figure 12. In the case of $R = 40$, it is seen that the copolymers can form well-ordered concentric strips when the PDI_A changes from 1.0 to 1.4, and the phase domain sequence from the boundary to the center remains A−B−A−B. However, the strips for both block A and B tend to become wider. Furthermore, the center phase domain

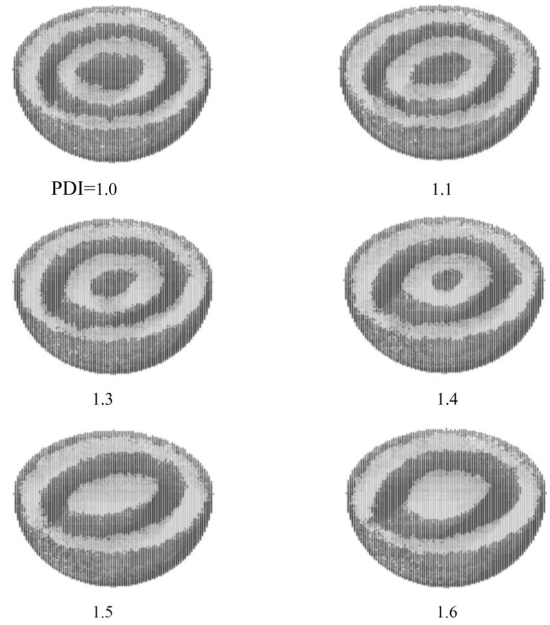

Figure 9. Snapshots of the polydisperse symmetric diblock copolymers confined within a spherical boundary condition. The radius of the spherical boundary is 46. The polydispersity indices are marked below the snapshots correspondingly.

decreases gradually with an increase in the PDI_A. When the circle radius is increased to 50, the phase domain sequence from the boundary to the center becomes A−B−A−B−A. The center phase domain decreases up to disappearance with an increase in the PDI_A to 1.4. As a result, a strip is lost and the center phase domain is replaced by block B. That is, the phase domain sequence from the boundary to the center becomes A−B−A−B in the case of $PDI_A = 1.4$. For the purpose of comparison, the self-assembly of the polydisperse asymmetric copolymers confined within two-concentric-circle boundaries was also studied. The distance between two circles ($R - r_0$) is kept as a constant. Figure 13 is the simulation results for different PDI_A and r_0. As expected, it is difficult for the polydisperse asymmetric diblock copolymers to form ordered structure within two-concentric-circle boundaries. The simulation results suggest that the circle confinement allows the polydisperse asymmetric copolymers to respond to the frustration by changing the size of the circular microdomain at the center of the system. Therefore, the copolymers are more likely to form concentric strip structures within a circle boundary.

Finally, comparing with the previous section, we can find that changing the chain length polydispersity and changing the

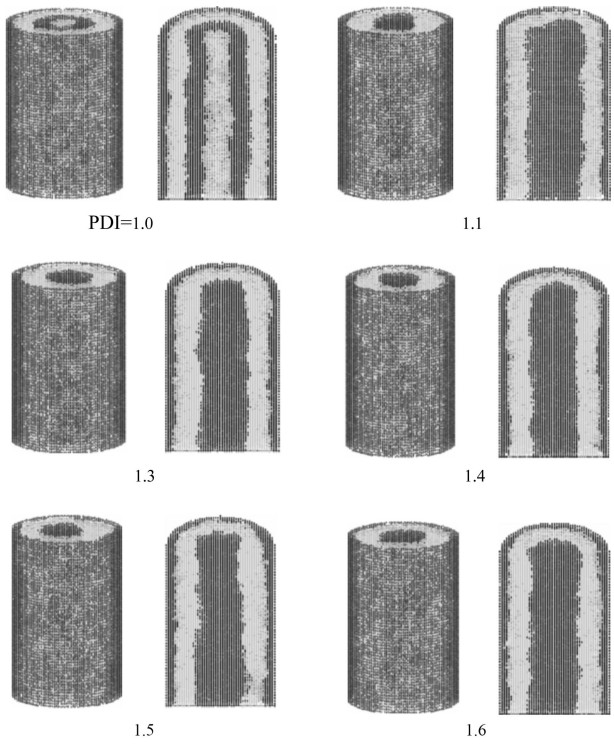

Figure 10. Snapshots and sectional counterparts of the polydisperse symmetric diblock copolymers confined within a cylindrical boundary condition. The radius of the cylindrical boundary is 24, and the length is 60. The polydispersity indices are marked below the snapshots correspondingly.

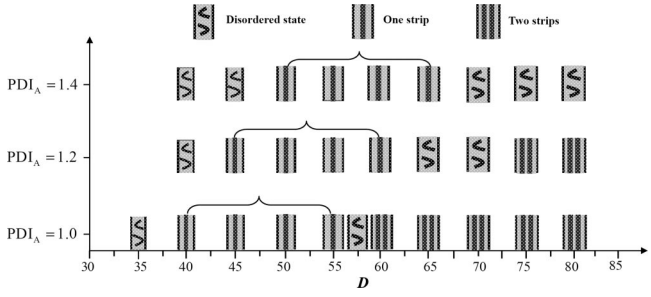

Figure 11. Diagram showing the structural variation with the PDI and wall width for polydisperse asymmetric diblock copolymers confined within two-parallel-wall.

block length polydispersity have a similar effect on the self-assembly structure for the confined polydisperse diblock copolymers.

4. Conclusions

Monte Carlo simulation was used to study the self-assembly of polydisperse diblock copolymers under various confined conditions. When the copolymers were confined within a two-parallel-wall, it was found that the ordered strip structures appeared alternately with the increase in wall width. Moreover, the wall width at which the ordered structure appeared tended to increase with an increase in the polydispersity index (PDI). On the other hand, the copolymers were more likely to form ordered concentric strip structures if the copolymers were confined within a circle boundary. The structure changed from an ordered concentric strip structure to a new ordered concentric strip structure with an increase in the PDI. In addition, the results showed that one strip was lost, and the center was occupied by the other component with an increase in the PDI. Similar results were obtained if the copolymers were confined in a spherical

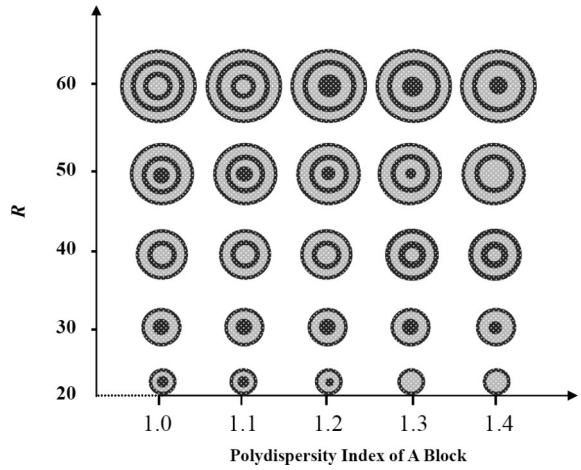

Figure 12. Diagram showing the structural variation with the PDI and circle radius (R) for polydisperse asymmetric diblock copolymers confined within a circle boundary.

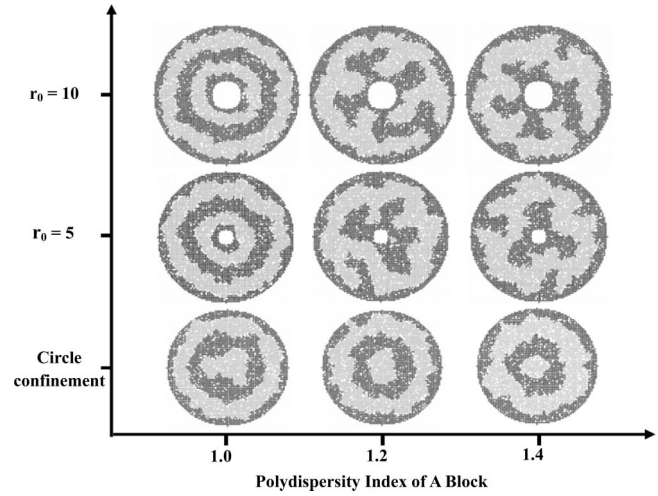

Figure 13. Snapshots of polydisperse asymmetric diblock copolymers confined within two-concentric-circle boundaries with different inside radius r_0 compared to the snapshots obtained in the circle boundary. The distance ($R - r_0$) between these two circle walls is 40. For the purpose of comparison, the simulation results for the circle confinement ($R = 40$) is given in this figure accordingly.

or cylindrical space. For comparison purposes, we kept the diblock chain length unchanged and instead changed the length of one block. The simulation results indicated that changing the block polydispersity had a similar effect on the structure formation of confined symmetric diblock copolymers; that is, the system could also change from an ordered concentric strip to a new well-ordered concentric strip structure with an increase in block polydispersity. The simulation results were well interpreted in terms of the frustration between the bulk lamellar repeat period and the confined spacing.

Acknowledgment. We are grateful for the financial support provided by the National Basic Research Program (2007CB808000) of China. Jiang W. thanks the Funds for Outstanding Young Investigators (50725312), Creative Research Groups (50621302), and the Major Program (20490220) provided by National Natural Science Foundation of China.

Supporting Information Available: Simulation results for the polydisperse diblock copolymer systems under period conditions (i.e., without confinement) and within the circle confinement. This material is available free of charge via the Internet at http://pubs.acs.org.

References and Notes

(1) Matsen, M. W.; Bates, F. S. *Macromolecules* **1996**, *29*, 7641.
(2) Hamley, I. W. *The Physics of Block Copolymers*; Oxford University Press: Oxford, UK, 1998.
(3) Geisinger, T.; Müller, M.; Binder, K. *J. Chem. Phys.* **1999**, *111*, 5241.
(4) Geisinger, T.; Müller, M.; Binder, K. *J. Chem. Phys.* **1999**, *111*, 5251.
(5) Wang, Q.; Yan, Q. L.; Nealey, P. F.; Pablo, J. J. D. *J. Chem. Phys.* **2000**, *112*, 450.
(6) He, X. H.; Song, M.; Liang, H. J.; Pan, C. Y. *J. Chem. Phys.* **2001**, *114*, 10510.
(7) Chen, P.; He, X. H.; Liang, H. J. *J. Chem. Phys.* **2006**, *124*, 104906.
(8) Yu, B.; Sun, P. C.; Chen, T. H.; Jin, Q. H.; Ding, D. T.; Li, B. H.; Shi, A.-C. *Phys. Rev. Lett.* **2006**, *96*, 138306.
(9) Feng, J.; Ruckenstein, E. *Macromolecules* **2006**, *39*, 4899.
(10) Feng, J.; Liu, H. L.; Hu, Y. *Macromol. Theory Simul.* **2006**, *15*, 674.
(11) Feng, J.; Ruckenstein, E. *J. Chem. Phys.* **2006**, *125*, 164911.
(12) Zhu, Y. T.; Jiang, W. *Macromolecules* **2007**, *40*, 2872.
(13) Wang, Q. *J. Chem. Phys.* **2007**, *126*, 024903.
(14) Chen, P.; Liang, H. J.; Shi, A.-C. *Macromolecules* **2007**, *40*, 7329.
(15) Yu, B.; Sun, P. C.; Chen, T. H.; Jin, Q. H.; Ding, D. T.; Li, B. H.; Shi, A.-C. *J. Chem. Phys.* **2007**, *127*, 114906.
(16) Yu, B.; Li, B. H.; Jin, Q. H.; Ding, D. T.; Shi, A.-C. *Macromolecules* **2007**, *40*, 9133.
(17) Xiao, X. Q.; Huang, Y. M.; Liu, H. L.; Hu, Y. *Macromol. Theory Simul.* **2007**, *16*, 166.
(18) Xiao, X. Q.; Huang, Y. M.; Liu, H. L.; Hu, Y. *Macromol. Theory Simul.* **2007**, *16*, 732.
(19) Kellogg, G. J.; Walton, D. G.; Mayes, A. M.; Lambooy, P.; Russell, T. P.; Gallagher, P. D.; Satija, S. K. *Phys. Rev. Lett.* **1996**, *76*, 2503.
(20) Xiang, H.; Shin, K.; Kim, T.; Moon, S. I.; McCarthy, T. J.; Russell, T. P. *Macromolecules* **2004**, *37*, 5660.
(21) Shin, K.; Xiang, H.; Moon, S. I.; Kim, T.; McCarthy, T. J.; Russell, T. P. *Science* **2004**, *306*, 76.
(22) Xiang, H.; Shin, K.; Kim, T.; Moon, S. I.; McCarthy, T. J.; Russell, T. P. *Macromolecules* **2005**, *38*, 1055.
(23) Xiang, H.; Shin, K.; Kim, T.; Moon, S. I.; McCarthy, T. J.; Russell, T. P. *J. Polym. Sci., Part B: Polym. Phys.* **2005**, *43*, 3377.
(24) Zhang, M.; Dobriyal, P.; Chen, J.-T.; Russell, T. P. *Nano Lett.* **2006**, *6*, 1075.
(25) Wu, Y. Y.; Cheng, G. S.; Katsov, K.; Sides, S. W.; Wang, J. F.; Tang, J.; Fredrickson, G. H.; Moskovits, M.; Stucky, G. D. *Nat. Mater.* **2004**, *3*, 816.
(26) Schichtel, T. E.; Binder, K. *Macromolecules* **1987**, *20*, 1671.
(27) Burger, C.; Ruland, W.; Semenov, A. N. *Macromolecules* **1990**, *23*, 3339.
(28) An, L. J.; Kou, X. C.; Ma, R. T.; Tang, X. Y. *Polymer* **1993**, *34*, 2989.
(29) Takenaka, M.; Hashimoto, T. *Phys. Rev. E* **1993**, *48*, R647.
(30) Yang, J.; Sun, Z. Y.; Jiang, W.; An, L. J. *J. Phys. Chem. B* **2002**, *106*, 11305.
(31) Fredrickson, G. H.; Sides, S. W. *Macromolecules* **2003**, *36*, 5415.
(32) Sides, S. W.; Fredrickson, G. H. *J. Chem. Phys.* **2004**, *121*, 4974.
(33) Jiang, Y.; Chen, T.; Ye, F. W.; Liang, H. J.; Shi, A.-C. *Macromolecules* **2005**, *38*, 6710.
(34) Cooke, D. M.; Shi, A.-C. *Macromolecules* **2006**, *39*, 6661.
(35) Ji, S. C.; Ding, J. D. *Langmuir* **2006**, *22*, 553.
(36) Gao, Z.; Eisenberg, A. *Macromolecules* **1993**, *26*, 7353.
(37) Luo, L.; Eisenberg, A. *Langmuir* **2001**, *17*, 6804.
(38) Choucair, A. A.; Kycia, A. H.; Eisenberg, A. *Langmuir* **2003**, *19*, 1001.
(39) Bendejacq, D.; Ponsinet, V.; Joanicot, M.; Loo, Y.-L.; Register, R. A. *Macromolecules* **2002**, *35*, 6645.
(40) Terreau, O.; Luo, L. B.; Eisenberg, A. *Langmuir* **2003**, *19*, 5601.
(41) Terreau, O.; Bartels, C.; Eisenberg, A. *Langmuir* **2004**, *20*, 637.
(42) Matsushita, Y.; Noro, A.; Iinuma, M.; Suzuki, J.; Ohtani, H.; Takano, A. *Macromolecules* **2003**, *36*, 8074.
(43) Noro, A.; Cho, D.; Takano, A.; Matsushita, Y. *Macromolecules* **2005**, *38*, 4371.
(44) Lynd, N. A.; Hillmyer, M. A. *Macromolecules* **2005**, *38*, 8803.
(45) Carmesin, I.; Kremer, K. *Macromolecules* **1988**, *21*, 2819.
(46) Larson, R. G.; Scriven, L. E.; Davis, H. T. *J. Chem. Phys.* **1985**, *83*, 2411.
(47) Larson, R. G. *J. Chem. Phys.* **1989**, *91*, 2479.
(48) Lu, J.; Yang, Y. *Sci. China A* **1991**, *11*, 1226.
(49) Metropolis, N.; Rosenbluth, A. W.; Rosenbluth, M. N.; Teller, A. H.; Teller, E. *J. Chem. Phys.* **1953**, *21*, 1087.

MA800702F